Pulmonary Artery Anatomical Characterization: Relevance to Pulmonary Artery Pressure Sensors

Hamza Zafar
University of Sheffield
Dharshan Neelam-Naganathan
University of Sheffield
Jennifer T Middleton
University of Sheffield
Dominic Rogers
Sheffield Teaching Hospitals NHS Foundation Trust
Andrew J Swift
University of Sheffield
Alexander Rothman (a.rothman@sheffield.ac.uk)
University of Sheffield
Sarah K Binmahfooz
University of Sheffield
Christian Battersby
University of Sheffield

Article

Keywords: Remote patient monitoring, heart failure, GDMT

Posted Date: May 26th, 2022

DOI: https://doi.org/10.21203/rs.3.rs-1643488/v1

Additional Declarations: No competing interests reported.

Version of Record: A version of this preprint was published at Scientific Reports on November 22nd, 2023.
See the published version at https://doi.org/10.1038/s41598-023-47612-9.

Abstract

In patients with heart failure, guideline-directed medical therapy improves outcomes and requires close patient monitoring. Pulmonary artery pressure monitors permit remote assessment of cardiopulmonary haemodynamics and facilitate early intervention that has been shown to decrease heart failure hospitalization. Pressure sensors implanted in the pulmonary vasculature are stabilized through passive or active interaction with the anatomy and communicate with an external reader to relay invasively measured pressure by radiofrequency. A body mass index (BMI) > 35 kg/m^2 and chest circumference >165 cm prevent use due to poor communication. Pulmonary vasculature anatomy is variable between patients and the pulmonary artery size, angulation of vessels and depth of sensor location from the chest wall in heart failure patients who may be candidates for pressure sensors remains largely unexamined.

This paper analyzes the size, angulation, and depth of the pulmonary artery at the position of implantation of two pulmonary artery pressure sensors: the CardioMEMS sensor typically implanted in the left pulmonary artery and the Cordella sensor implanted in the right pulmonary artery. Thirty-four computed tomography pulmonary angiograms from heart failure patients were selected for analysis. Distance from the bifurcation of the pulmonary artery to the implant site was shorter for the right pulmonary artery (4.55 ± 0.64 cm vs 7.4 ± 1.3 cm) and vessel diameter at the implant site was larger (17.15 ± 2.87 mm vs 11.83 ± 2.30 mm). Link distance (length of the communication path between sensor and reader) was shorter for the left pulmonary artery (9.40 ± 1.43 mm vs 12.54 ± 1.37 mm). Therefore, the detailed analysis of pulmonary arterial anatomy using computed tomography pulmonary angiograms may alter the choice of implant location to reduce the risk of sensor migration and improve readability by minimizing sensor to reader link distance.

Background

Congestive heart failure (CHF) is a chronic condition associated with significant symptoms and frequent episodes of decompensation that lead to frequent healthcare interactions, hospitalization, and premature death.[1–2] Prognosis of heart failure patients remains poor, despite the development of effective pharmacological and non-pharmacological interventions.[3–8] Increased left ventricular filling pressures have been shown to precede symptoms of decompensation, making accurate measurements of these changes a priority in clinical management.[9–11] Historically, repeated measurements of cardiopulmonary haemodynamics via invasive right heart catheterization (RHC) have been used to guide therapeutic escalation, transition to advanced therapies and determine eligibility and inform the timing of heart transplantation.[12] However, repeated measurements are limited due to the invasive nature of the procedure. The development of implanted pressure monitoring devices offers the unique opportunity to monitor clinical markers of worsening disease in patients with CHF, allowing for more timely interventions and then gauging the effect of the interventions on haemodynamics in real-time while the patient is in the community for treatment optimization. This paper analyses the size, angulation, and depth of the pulmonary artery at the position of implantation of two pulmonary artery pressure sensors: the

CardioMEMS sensor typically implanted in the left pulmonary artery and the Cordella sensor implanted in the right pulmonary artery (Fig. 1).

The accuracy and reliability of the pulmonary artery pressure (PAP) readings depend critically on the position of the sensor in the pulmonary vasculature and its relationship to the interrogating device on the anterior chest wall or back. Pressure sensors implanted in the pulmonary vasculature are stabilized through passive or active interaction with the anatomy and communicate with an external reader to wirelessly transmit the invasively measured hemodynamic data using radiofrequency.[13] Pulmonary vasculature anatomy is variable between patients and the size, angulation of vessels, and depth of sensor location from the chest wall is largely unexamined. Sensor implant stability is crucial for accurate readings. However, sensor migration is most likely to happen during the implant procedure especially if implanted in unfavourable anatomy or if it jumps proximally during implant. However, the mechanisms of late implant migration are still not as clear. Possible mechanisms include placement in a larger than recommended pulmonary artery, a more horizontal rather than vertical orientation of the artery, or an artery which is proximally located.[14–15]

The present study describes the spatial orientation and PA morphology in a population of patients with heart failure to highlight key differences in anatomy relevant to PAP monitor implantation, orientation, link distance and clinical use.

Methods

Study Population

Thirty-eight CT pulmonary angiogram (CTPA) scans obtained at the University of Sheffield database (UK) were analyzed to evaluate the dimensions and metrics of the PA. The eligible patients were men or women over 18 years with a diagnosis of New York Heart Association (NYHA) class I-IV HF with reduced or preserved ejection fraction and had no contraindications to CTPA. From this, 34 CT scans were chosen for PA characterization analysis based on the quality of images and measurability at distal segments. The sample consisted of 53% males and 47% females.

CT Pulmonary Angiogram Methods

CT pulmonary angiogram scans acquired from the University of Sheffield were done on light-speed 64-slice MDCT scanners. The parameters of the imaging included 100 mA with automated dose reduction, 120 kV, pitch 1, with a rotation time of 0.5s and 0.625 collimation. The field of view used was 400 mm x 400 mm with an acquisition matrix of 512 x 512. For the imaging, 100 ml of Ultravist and Bayer IV contrast agents were used and administered at 5mL/s. High-resolution CT scans (HRCTs) were reconstructed using the contrast-enhanced acquisitions with 1.25 mm collimation from the apex of the lung to the diaphragm and the methods were carried out in the accordance with the relevant published guidelines.[16]

Analysis methods

A three-dimensional (3D) model of the PA was constructed through MIMICS medical imaging software using imported patient DICOM images. A “mask” was created in MIMICS to highlight the area of interest in the images. The “mask” was then split to help differentiate PA from extraneous highlighted segments.

The PA was studied in axial, coronal, and sagittal views to allow for more accurate measurements. In the axial view, axes were aligned such that the coronal axis ran parallel to the RPA wall and the sagittal axis lay perpendicular to the RPA wall. In the coronal view, axes were aligned such that the axial axis ran parallel to the RPA wall and the sagittal axis lay perpendicular to the RPA wall. In the sagittal view, the coronal and axial axes intersect at the centre of the circular RPA outline.

The PA metrics evaluated in this study were vessel diameter for both RPA and left pulmonary artery (LPA), the distance of the segment length from the zone where the implantable sensor would be placed in the vessels to the MPA bifurcation, the distance between the sensor and the sensor reader, or what’s called the link distance, the angle of the RPA downturn and the chest circumference of each patient.

The LPA and RPA were divided into 3 zones and the diameter of each zone was determined for analysis. Zone 1 (Proximal) was defined as the section on the RPA and LPA between the main PA bifurcation and the first branch of the RPA and LPA and proximal to the sensor deployment zone. Zone 2 (Sensor) was defined as the section distal to Zone 1 where the Cordella sensor (RPA) and CardioMEMS (LPA) are deployed. Zone 3 (Distal) was defined to be 2cm distal to Zone 2 (Fig. 2A). The diameter of each zone in the RPA was calculated as the average of the horizontal and vertical diameters of each zone which were measured along the axial axis in sagittal view and coronal axis in sagittal view, respectively. The diameter of each zone in the LPA was measured diagonally in between the sagittal and coronal sections in the axial view. For the LPA, only one diameter measurement was constructed instead of the average of two different diameters from two different planes respectively. The segment length from the MPA bifurcation to Zone 2 of each vessel was measured along the coronal axis in axial view (Fig. 3A**).** The chest circumference was also measured in axial view at PA level using a spline that went along the outer chest wall. The length of the spline was recorded as chest circumference. The link distance (LD) was recorded as the distance from the implantable sensor in each vessel to the skin surface (where a reader device will be located). The Cordella sensor was placed in the RPA at the downturn and CardioMEMS in the LPA. The link distance for the RPA was recorded as the distance from the sensor to the reader that is on the anterior chest surface. The link distance of the LPA was measured as the distance from the sensor to the closest point on the posterior surface of the back of the patient where they will be placed (Fig. 4A, 4C). The RPA downturn is defined as the location in the RPA downstream of the apical bifurcation where the interlobar artery typically turns downward and posterior before further branching into a series of basal arteries feeding the lower lung lobes. The angle of this downturn was measured for analysis (Fig. 5A**).**

The study was conducted in accordance with ASPIRE ((Assessing the Severity of Pulmonary Hypertension In a Pulmonary Hypertension REferral Centre)) code of ethics approved by Yorkshire and

The Humber – Sheffield Ethics Research committee REC:16/YH/0352 and the processing of data complied with the terms of informed consent from the data subjects. The methods were carried out in accordance with the declaration of Helsinki.

Statistical Analysis

Statistical analysis was performed using Microsoft Excel (Microsoft Inc., Redmond, WA, USA). Through this, the mean, median, standard deviation, minimum and maximum were determined. The coefficient of variation (CV) was also calculated to help compare metrics of different nature with different units as it is a statistical measure of the relative dispersion of data points in a data series around a mean.

Results

Thirty-eight heart failure patients at the Sheffield Teaching Hospitals NHS Trust were analysed, and 34 CT scan images were chosen for 3D reconstruction based on the quality of images and measurability of pre-selected distal segments. Patients were 53% male and had a mean age of 74.8 years with a mean ejection fraction of 47.1%. Nearly half of the patients were NYHA class III and IV (47.2%), 29.4% had COPD, 41.4% had hypertension, and 32.2% had atrial fibrillation (Table 1**).** The distance from the bifurcation of the main PA to the sensor was as follows: RPA (4.55 ± 0.64 cm) and LPA (7.4 ± 1.3 cm) (Fig. 3B**)**. As seen in the figure, the LPA distance from the site of implantation to the MPA bifurcation is greater and has greater variability compared to RPA.

Table 1
Demographic characteristics, comorbidities, and NYHA classification of 34 patients involved in this research project.

Patient Characteristics	Analysed cohort (n)
Implanted Population (n)	34
Demographics	
Age (years), mean, range	74.8 (29.0–92.0)
Male, % (n)	53.0 (18)
Female, % (n)	47.1 (16)
Asian race, % (n)	2.9 (1)
Caucasian race, % (n)	97.1 (33)
Comorbidities	
Myocardial Infarction, % (n)	8.8 (3)
Diabetes Mellitus, % (n)	23.5 (8)
Coronary Artery Disease, % (n)	44.1 (15)
Hypertension, % (n)	41.1 (14)
Atrial flutter/fibrillation, % (n)	32.2 (11)
COPD, % (n)	29.4 (10)
Ejection Fraction mean (range)	47.1 (24.0–66.0)
NYHA Classification	
NYHA Classification I, % (n)	20.5 (7)
NYHA Classification II, % (n)	32.3 (11)
NYHA Classification III, % (n)	41.4 (14)
NYHA Classification IV, % (n)	5.8 (2)
.	

The vessel diameters were as follows: RPA proximal (25.75 ± 4.65 mm), RPA sensor (17.15 ± 2.87 mm), and RPA distal (12.79 ± 2.92 mm). LPA proximal (26.00 ± 4.05 mm), LPA sensor (11.83 ± 2.30 mm), and LPA distal (7.39 ± 1.55 mm) (Fig. 2B). As seen in the figure, the LPA zone diameter decreased faster than the RPA diameters even though the most proximal diameters are almost identical. As a result, in Zone 2 where the implants are placed, the RPA diameter is larger than the LPA diameter.

Link distance was as follows: for the Cordella sensor to the reader on the anterior chest (12.54 ± 1.37 mm) and the CardioMEMS sensor to the reader on the posterior back (9.40 ± 1.43 mm) (Fig. 4B). Link Distance correlated with chest circumference, as one would expect, with the coefficient of determination for both RPA and LPA nearing 1 (R^2 = 0.99 for both RPA and LPA) (Fig. 4D). The downturn angle of the RPA (Cordella sensor) measured 135.5 ± 8.2 degrees across all patients. Given that the Cordella sensor is a landmark-based design, we sought to examine the coefficient of variation in sensor location (angle vs diameter). As shown in Fig. 5B, the CV for the RPA downturn angle is 5% whereas the CV for the RPA diameter and LPA diameter are 17% and 19%, respectively meaning the angle of the downturn is more consistent across this patient population than vessel diameter at the level of LPA Zone 2 and a detailed stepwise methodology and quality checks are further described in the online Supplementary Document.

Discussion

Heart failure remains a cause of significant morbidity and mortality and places a large burden on healthcare expenditure.[12] With the development of PAP pressure sensors, heart failure patient monitoring and GDMT interventions are possible in real-time, bridging the gap between clinic visits, allowing for proactive remote monitoring to reduce HF-related readmissions and mortality.[17]

Both the CardioMEMS and Cordella devices use micro-electromechanical systems (MEMS) and radiofrequency technology to accurately transduce pressure and communicate to their respective readers. MEMS can act as sensors, receiving information from their environment and providing an electrical output signal for an external reader. The strength of the communication signal is altered by the alignment and length of the path between the sensor and the reader. Key design features influence implant location with implications for device use and accurate, accessible home readings. The CardioMEMS sensor resides in the lumen of the LPA and PAP is captured by the patient while lying supine on the reader pillow. The Cordella sensor resides against the anterior wall of the RPA and PAP is captured using a hand-held reader from either the seated or supine position. The proximal anchor of the Cordella sensor uses the principle of outward radial force to interact with and fix to the vessel wall. The pre-selected target implant location in the RPA should measure 12–26 mm to allow for proper proximal anchor engagement.[18] The vessel diameter at the site of the sensor deployment was 17.15 ± 2.87 mm in this study, well within the range of the design specifications. The distal anchor has a parent shape-set configuration approximately orthogonal to the sensor body. When deployed, the distal anchor deflects distally and, due to the shape memory effect of nitinol, exerts a bending force in the direction of its parent shape-set, towards the vessel wall, securing the sensor in place. The angle of the downturn of the RPA was 135.5 ± 8.2 degrees in this study and indicates that there is adequate strain put on the anchor across this patient population to exert a sufficient bending force to secure the anchor in place and control rotation. Fixing the sensor at a known landmark, the downturn of the RPA has potential advantages including orientation and stabilization of the sensor and standardization of implanting.[14,15] Both anchors of the CardioMEMS sensor use the principle of outward radial force to interact and fix to the vessel wall. The pre-selected target vessel is within the lower lobe of either lung with the vessel directed towards the feet and back, the vessel diameter

is ≥ 7 mm and has < 30-degree angulation where the body of the sensor will be placed, and the vessel diameter is 5–8 mm where the distal anchor will be placed.[19] The vessel diameter at the site of sensor body deployment was 11.83 ± 2.30 mm, well within the range of the implant recommendations. The RPA sensor location provides a sensor-to-anterior chest link distance of 12.54 ± 1.37 mm which permits signal transmission detection from the anterior chest with a hand-held reader in contrast to supine, posterior readings with the LPA implant sensors. Anterior chest wall permits reading in the supine and upright position. Furthermore, the route of implantation is feasible from the groin or IJV with either device. Jugular implantation of CardioMEMS has been demonstrated to be safe and feasible.[20]Additionally, the opportunity to take standing and ambulatory readings with the hand-held reader opens the possibility to assess patient haemodynamics while ambulating, in the clinic or in the home environment.

Conclusion

In this paper left and right pulmonary arteries were characterized as the locations for the Abbott CardioMEMS and Cordella PA sensors. The CardioMEMS sensor has a “diameter-based” design and is typically implanted in the LPA where anatomy permits. The Cordella sensor has a “landmark-based” design meant to be deployed in the RPA, distal to the apical bifurcation, where the interlobar artery typically turns downward and posterior. This landmark varied less with respect to vessel diameter and location from the main bifurcation of the PA, respectively. The downturn angle where the distal anchor is deployed was also consistent across this patient population. Furthermore, the Cordella sensor is designed to be implanted as opposed to the arterial wall with two different anchor mechanisms to allow for increased endothelialization and reduced sensor migration. Across the study population, chest circumference correlated with sensor-reader link distance with the Cordella sensor having a smaller link distance with respect to the anterior chest allowing for front-sided readings with a hand-held reader. The CardioMEMS sensor has a smaller link distance to the patient’s back, consistent with the design of the reader pillow. Analysis of pulmonary vasculature anatomy with respect to PA diameter, angulation of vessels, and depth of sensor location prior to PAP sensor implantation may contribute to device choice and inform implant strategy.

Abbreviations

PAH	Pulmonary Arterial Hypertension
PAP	Pulmonary Artery Pressure
CHF	Congestive Heart Failure
RHF	Right Heart Failure
LV	Left Ventricle
HFpEF	Heart Failure with Preserved Ejection Fraction
CHFS	Cordella Heart Failure System
GDMT	Guideline Directed Medical Therapy
CT	Computerized Tomography
MDCT	Multidetector Computerized Tomography
MEMS	Micro-ElectroMechanical Systems
HRCT	High-Resolution Computerized Tomography
3D	3-Dimensional
DICOM	Digital Imaging and Communications in Medicine
PA	Pulmonary Artery
RPA	Right Pulmonary Artery
LPA	Left Pulmonary Artery
CFD	Computational Fluid Dynamics
TA	Truncus Anterior
HF	Heart Failure
IJV	Internal Jugular Vein
NYHA	New York Heart Association

Declarations

Acknowledgements:

None

References

1. Bleumink GS, Knetsch AM, Sturkenboom, MCJM, et al. Quantifying the heart failure epidemic: prevalence, incidence rate, lifetime risk and prognosis of heart failure. The Rotterdam Study. *Eur Heart J.* 2004; 25(18):1614-9
2. Roger VL, Go AS, Lloyd-Jones DM, et al. Heart Disease and Stroke Statistics-2012 Update: A Report from the American Heart Association. *Circulation* 2012; 125(1):e2-e220
3. Stewart S, MacIntyre K, Hole DJ, et al. More 'malignant' than cancer? Five-year survival following a first admission for heart failure. *Eur J Heart Failure* 2001; 3(3):315-22
4. Ammar KA, Jacobsen SJ, Mahoney DW, et al. Prevalence and prognostic significance of heart failure stages: application of the American College of Cardiology/American Heart Association heart failure staging criteria in the community. *Circulation* 2007; 115(12):1563-70
5. Landolina M, Perego GB, Lunati M, et al. Remote monitoring reduces healthcare use and improves the quality of care in heart failure patients with implantable defibrillators: the evolution of management strategies of heart failure patients with implantable defibrillators (EVOLVO) study. *Circulation* 2012; 125(24):2985-92
6. Bui AL, Horwich TB, Fonarow GC. Epidemiology and risk profile of heart failure. *Nat Rev* Cardiol 2011; 8(1):30-41
7. Crespo-Leiro MG, Anker SD, Maggioni AP, et al. European Society of Cardiology Heart Failure Long-Term Registry (ESC-HF-LT): 1-year follow-up outcomes and differences across regions. *Eur J Heart Fail* 2016; 18(6):613–25
8. Bueno H, Ross JS, Wang Y, et al. Trends in the length of stay and short-term outcomes among Medicare patients hospitalized for heart failure, 1993-2006. *JAMA* 2010; 303(21):2141-7
9. Mottram PM, Marwick TH. Assessment of diastolic function: what the general cardiologist needs to know. *Heart* 2005; 91(5):681-95
10. Desai AS, Stevenson LW. Rehospitalization for Heart Failure. Predict of Prevent? *Circulation* 2012; 126(4):501-6
11. Zile MR, Bourge RC, Bennett TD, et al. Application of Implantable Hemodynamic Monitoring in the Management of Patients With Diastolic Heart Failure: A Subgroup Analysis of the COMPASS-HF Trial. *J Card Fail* 2008; 14(10):816-23
12. McDonagh TA, Metra M, Adamo M, et al. 2021 ESC Guidelines for the diagnosis and treatment of acute and chronic heart failure. *Eur Heart J* 2021;42(36):3599-3726
13. Verdejo HE, Castro PF, Concepcion R, et al. Comparison of a radiofrequency-based wireless pressure sensor to swan-ganz catheter and echocardiography for ambulatory assessment of pulmonary artery pressure in heart failure. *J Am Coll Cardiol.* 2007;50(25):2375-82
14. Singh R, Scarfone S, Zughaib M. Wedged Sensor in Distress? Lessons Learned from Troubleshooting Dampened Transmitted PA Waveforms of a CardioMEMS Device. *Case Rep Cardiol* 2020; 2020:3856940

15. Rali AS, Shah Z, Sauer A, et al. Late Migration of CardioMEMS™ Wireless Pulmonary Artery Hemodynamic Monitoring Sensor. *Circ Heart Fail* 2017; 10(4):e003948
16. Swift AJ, Dwivedi K, Johns C, et al. Diagnostic accuracy of CT pulmonary angiography in suspected pulmonary hypertension. *Eur Radiol* 2020; 30:4918-4929
17. Wand AL, Russell SD, Gilotra NA. Ambulatory Management of Worsening Heart Failure: Current Strategies and Future Directions. *Heart International.* 2021;15(1):49-53
18. Endotronix Incorporated. *Cordella™ Pulmonary Artery Sensor System: Cordella™ Sensor and Delivery System Instructions for Use* 2018
19. Abbott Laboratories. *Manuals and Technical Resources.* Available from: https://www.cardiovascular.abbott/us/en/hcp/products/heart-failure/pulmonary-pressure-monitors/cardiomems/manuals-and-resources.html [Accessed 3 August 2021]
20. Middleton, J., Zafar, H., Kiely, David. G., & Rothman, A. (2021). 124 Comparing the safety and feasibility of implanting pulmonary artery pressure monitors via the internal jugular vein compared to standard femoral venous access in patients with pulmonary arterial hypertension. *Heart Failure*, A93.1-A93. https://doi.org/10.1136/heartjnl-2021-BCS.121

Figures

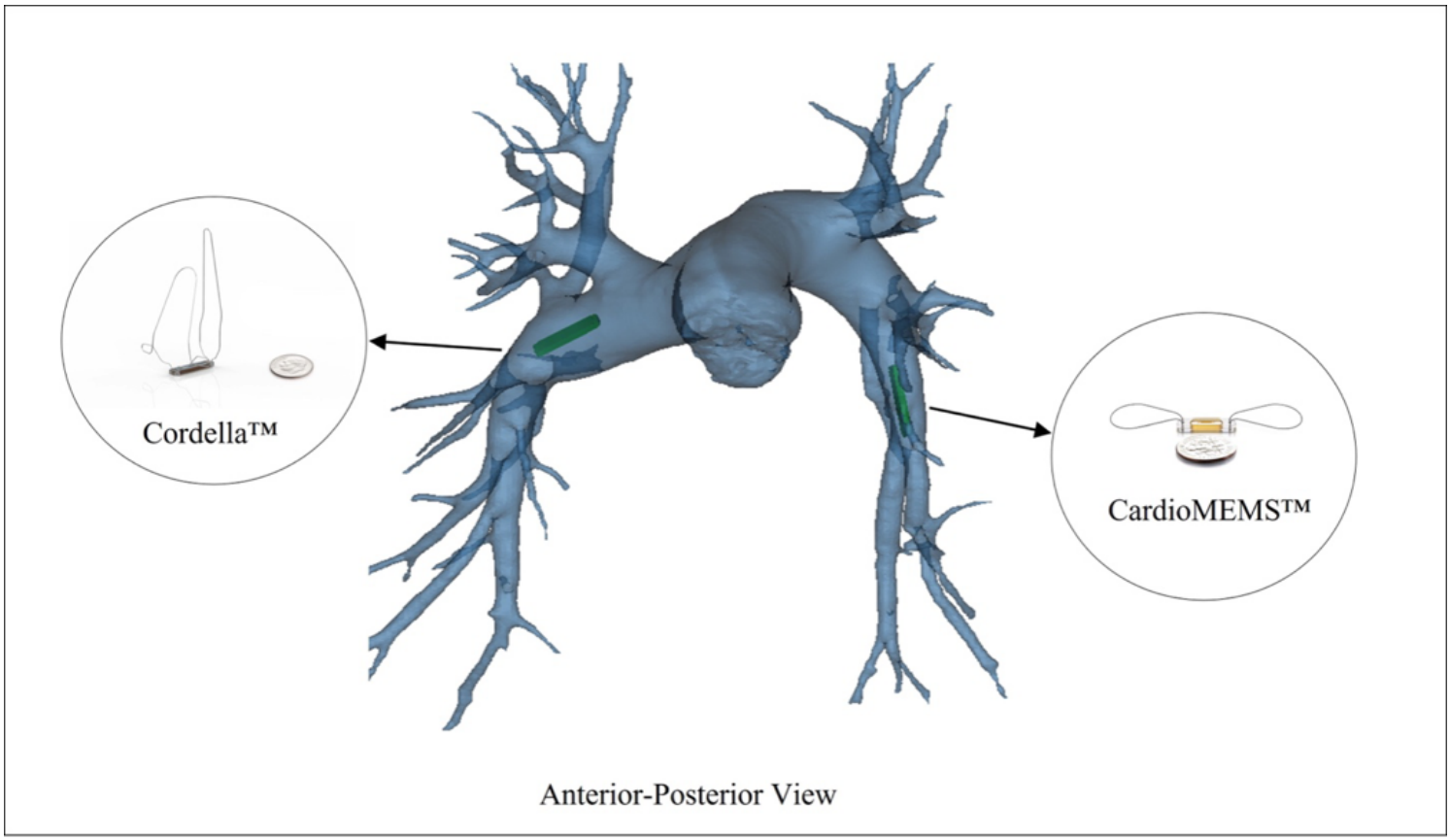

Figure 1

Pulmonary arterial anatomy depicting standard CardioMEMS^{TM} implant location in the LPA and fixed Cordella^{TM} implant location in the RPA

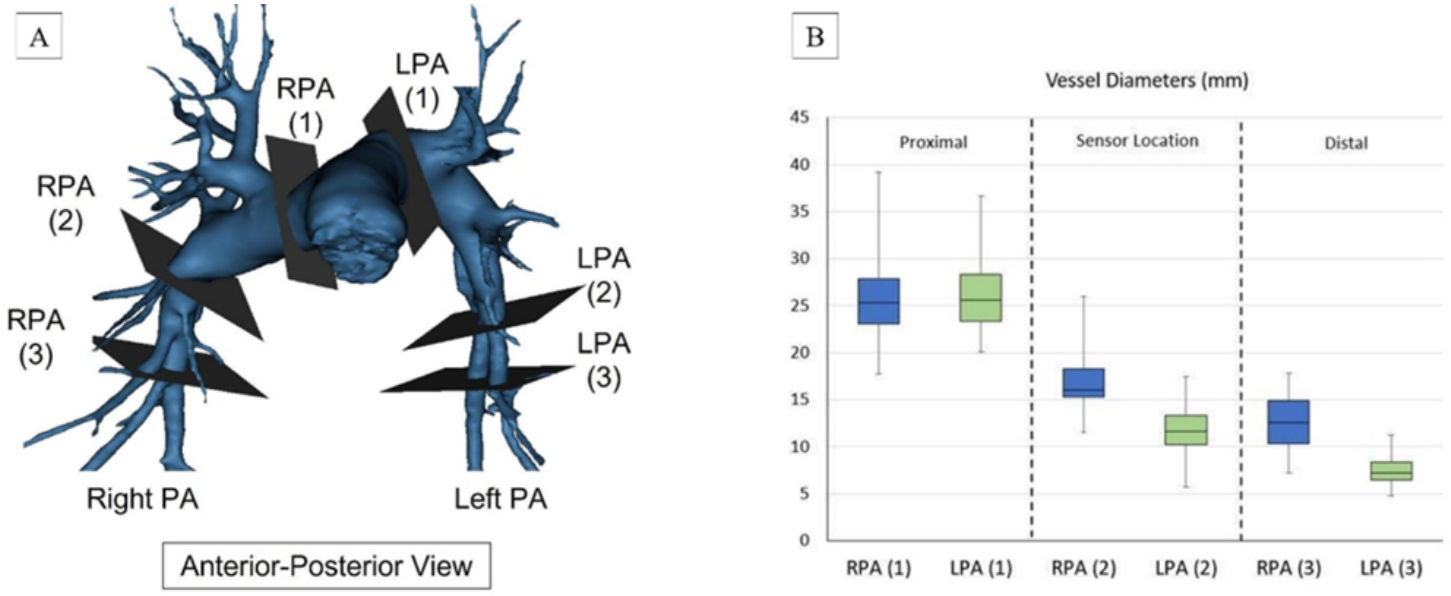

Figure 2

2A: RPA and LPA analysis zones. Zone 1 represents the proximal pulmonary artery zone between the main bifurcation and the first branch. Zone 2 represents the sensor deployment zone, and Zone 3 represents the zone distal deployment zone at the location of the distal sensor anchor for each device.

2B: Mean and standard deviation diameter (mm) of each zone for RPA and LPA.

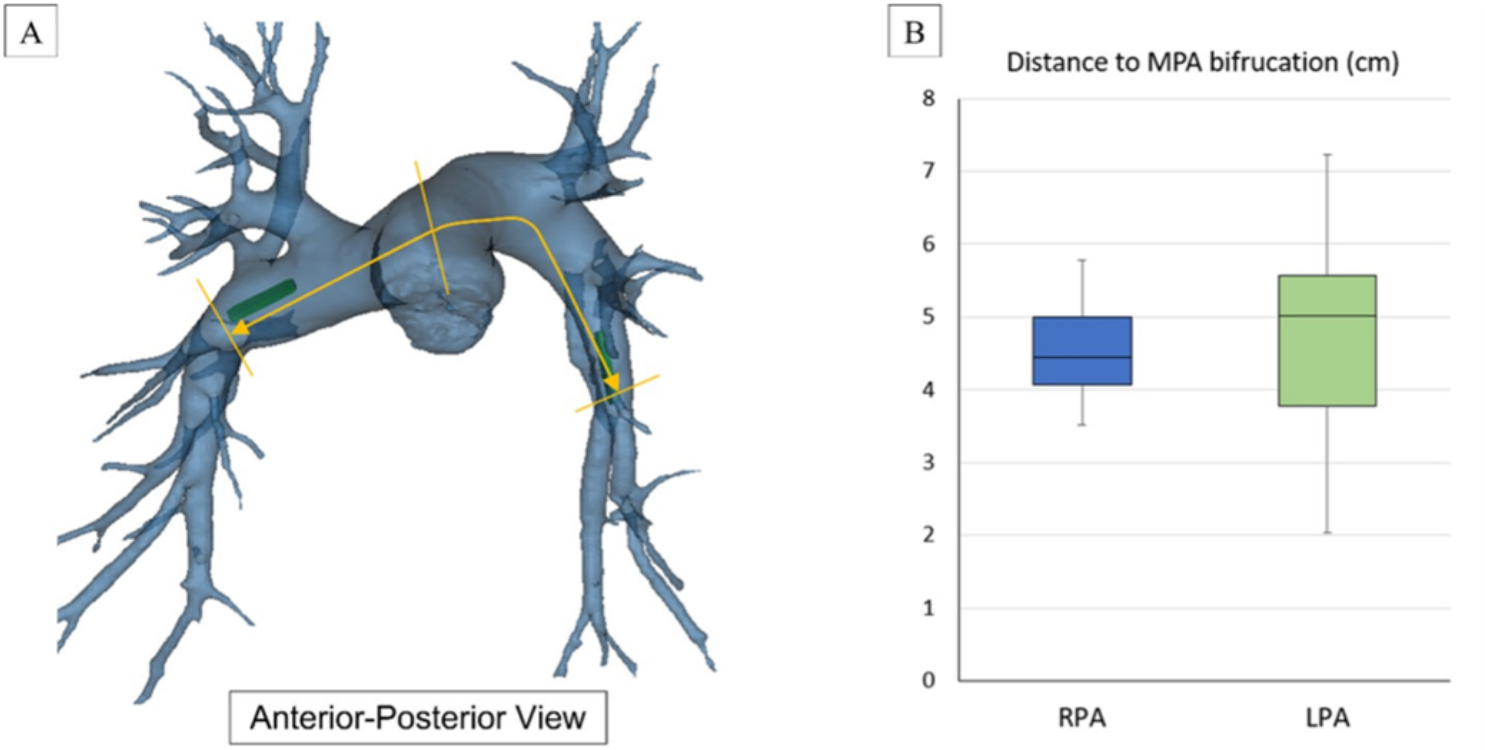

Figure 3

3A: Segment along which main PA bifurcation to sensor deployment zone for LPA and RPA were measured.

3B: Mean and standard deviation distance (mm) from main PA bifurcation to sensor deployment zone for LPA and RPA.

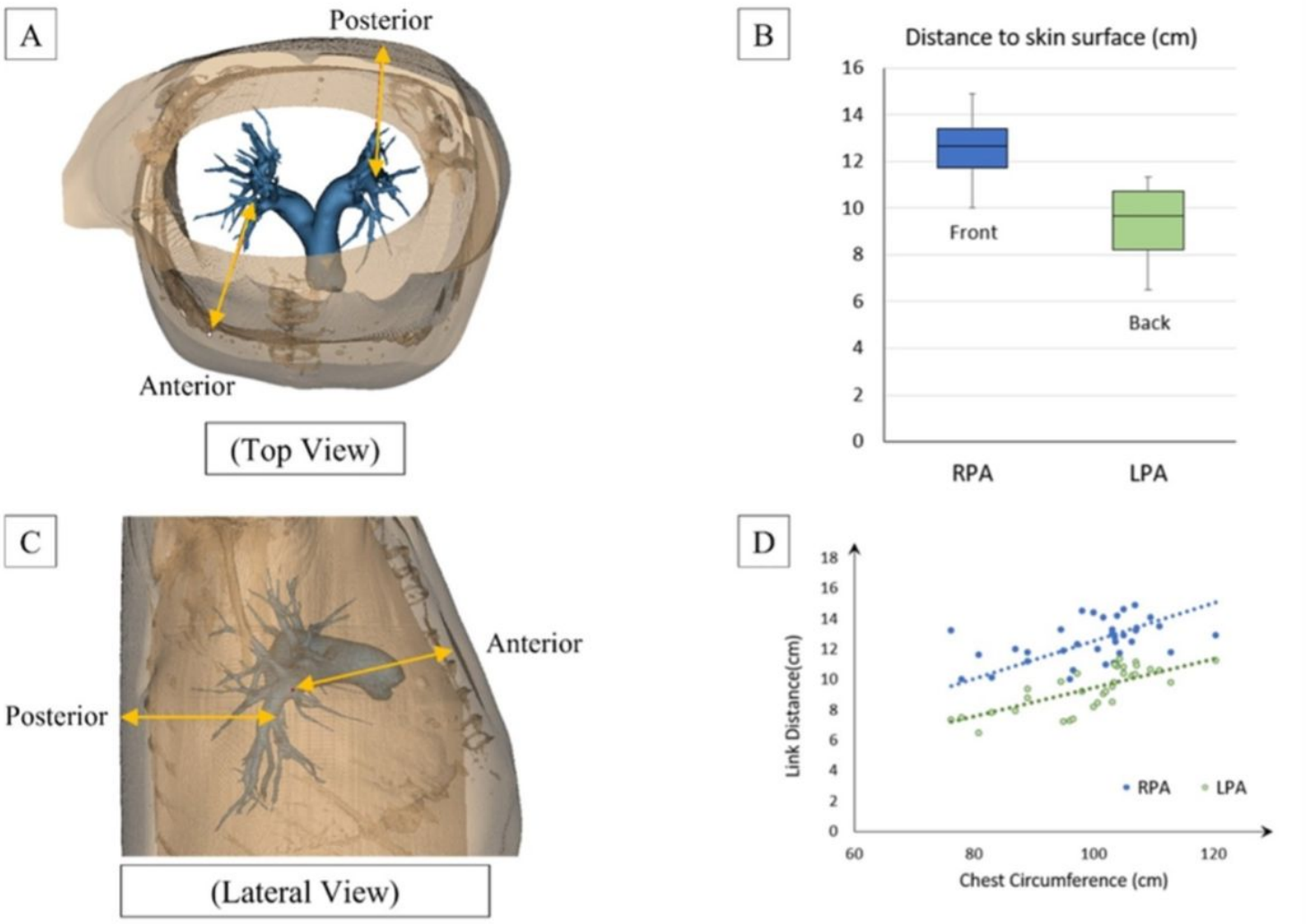

Figure 4

Link distance for Cordella^{TM} (Anterior) and CardioMEMS^{TM} (Posterior) as depicted in an axial view**. Figure 4B:** Link distance (cm) for both Cordella^{TM} (RPA-Front) and CardioMEMS^{TM} (LPA-Back)**. Figure 4C:** Link distance for Cordella^{TM} (Anterior) and CardioMEMS^{TM} (Posterior) as depicted in a lateral view**. Figure 4D:** Correlation plot for chest circumference vs link distance.

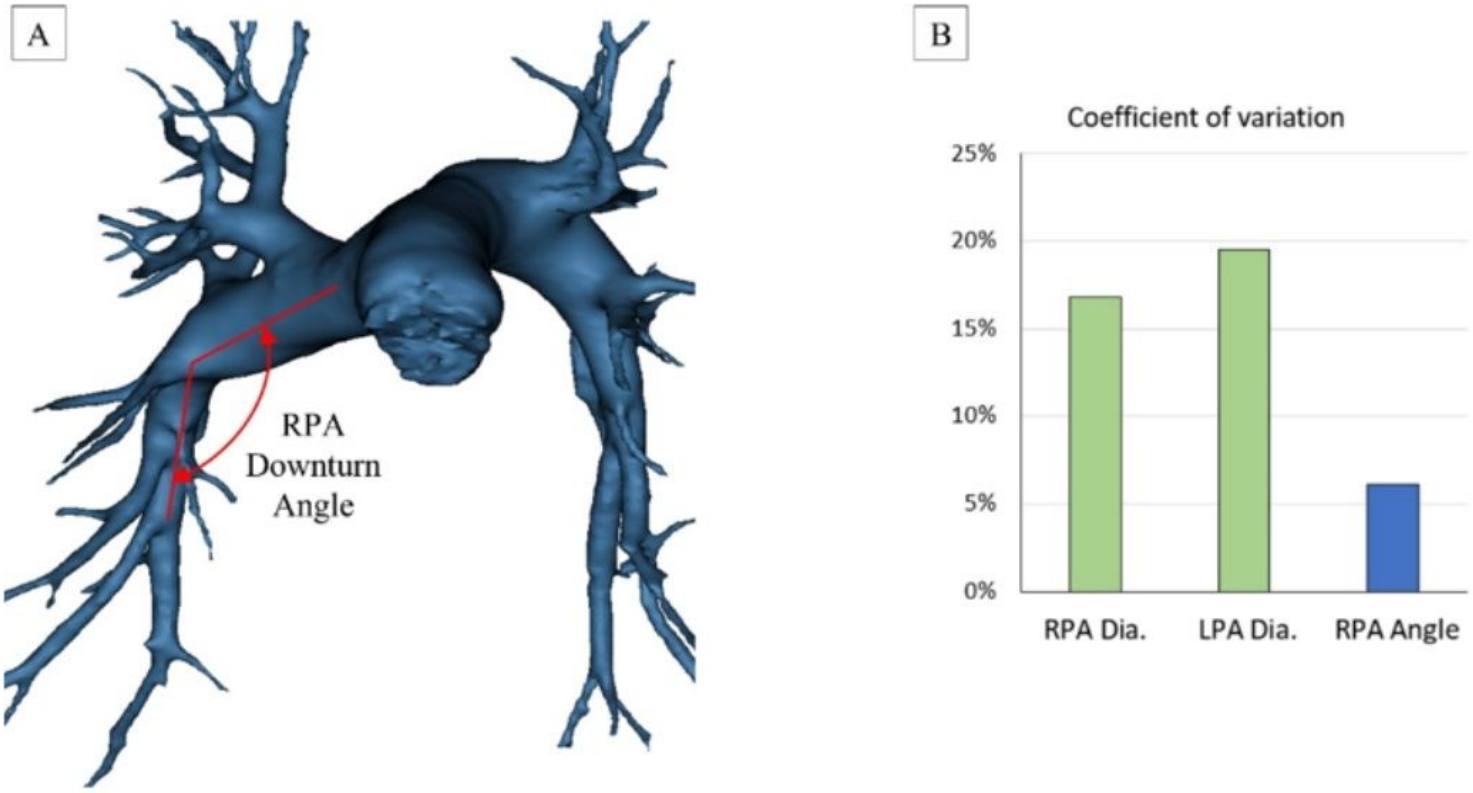

Figure 5

5A: Location of the downturn angle in the RPA downstream of the apical bifurcation where the interlobar artery typically turns downward and posterior before further branching into a series of basal arteries feeding the lower lung lobes. **Figure 5B:** Coefficient of variation RPA and LPA diameter at the location of sensor deployment and the RPA angle

Supplementary Files

This is a list of supplementary files associated with this preprint. Click to download.

- OnlineSupplementPulmonaryArteryAnatomical18052022Characterization.docx